

Relative contributions of “pressure pump” and “peristaltic pump” to gastric emptying

K. INDIRESHKUMAR,¹ JAMES G. BRASSEUR,¹ HENRYK FAAS,² GEOFFREY S. HEBBARD,³ PATRIK KUNZ,² JOHN DENT,⁴ CHRISTINE FEINLE,³ MEIJNG LI,¹ PETER BOESIGER,² MICHAEL FRIED,³ AND WERNER SCHWIZER³

¹Department of Mechanical Engineering, Pennsylvania State University, University Park, Pennsylvania 16802; ²Department of Biomedical Engineering and Medical Informatics, Swiss Federal Institute of Technology, Zurich; ³Department of Gastroenterology, University Hospital, Zurich, Switzerland; and ⁴Division of Gastroenterology, Royal Adelaide Hospital, Adelaide, Australia

Indireskumar, K., James G. Brasseur, Henryk Faas, Geoffrey S. Hebbard, Patrik Kunz, John Dent, Christine Feinle, Meijing Li, Peter Boesiger, Michael Fried, and Werner Schwizer. Relative contributions of “pressure pump” and “peristaltic pump” to gastric emptying. *Am J Physiol Gastrointest Liver Physiol* 278: G604–G616, 2000.—The relative contributions to gastric emptying from common cavity antroduodenal pressure difference (“pressure pump”) vs. propagating high-pressure waves in the distal antrum (“peristaltic pump”) were analyzed in humans by high-resolution manometry concurrently with time-resolved three-dimensional magnetic resonance imaging during intraduodenal nutrient infusion at 2 kcal/min. Gastric volume, space-time pressure, and contraction wave histories in the antropyloroduodenal region were measured in seven healthy subjects. The subjects fell into two distinct groups with an order of magnitude difference in levels of antral pressure activity. However, there was no significant difference in average rate of gastric emptying between the two groups. Antral pressure history was separated into “propagating high-pressure events” (HPE), “nonpropagating HPEs,” and “quiescent periods.” Quiescent periods dominated, and average pressure during quiescent periods remained unchanged with decreasing gastric volume, suggesting that common cavity pressure levels were maintained by increasing wall muscle tone with decreasing volume. When propagating HPEs moved to within 2–3 cm of the pylorus, pyloric resistance was found statistically to increase with decreasing distance between peristaltic waves and the pylorus. We conclude that transpyloric flow tends to be blocked when antral contraction waves are within a “zone of influence” proximal to the pylorus, suggesting physiological coordination between pyloric and antral contractile activity. We further conclude that gastric emptying of nutrient liquids is primarily through the “pressure pump” mechanism controlled by pyloric opening during periods of relative quiescence in antral contractile wave activity.

gastric motility; peristalsis; pressure wave; contraction wave; pump; mechanics

ALTHOUGH ANIMAL STUDIES indicate that gastric emptying is often pulsatile and that the pylorus is important in regulating the rate of gastric emptying (1, 13, 20, 21), the patterning of antral motor and pressure events, their coordinations with pyloric opening, and their relative contributions to gastric emptying in humans are not well understood. For example, intermittent transpyloric flow could, in principle, be created by intermittent increases in antral pressure in the presence of relatively constant pyloric resistance or by intermittent pyloric opening in the presence of a relatively constant antroduodenal pressure difference ($P_A - P_D$). Alternatively, gastric emptying could, in principle, be controlled more intelligently by neuromuscular coordination (3), or discoordination (14), of pyloric opening, with phasic increases in transpyloric pressure difference induced by antral contractile activity. The relative contributions of common cavity and phasic transpyloric pressure differences, the role of the pylorus in regulating transpyloric flow, and the variations in these components with meal composition and volume have not been well delineated in humans (4, 8). With recognition that the direction and magnitude of transpyloric flow follow, from basic fluid mechanical considerations (2, 11, 12), from transpyloric pressure differences across an open pylorus, there is much gastric physiology to be learned by detailed quantitative analysis of coordinated pressure and imaging data.

Mechanically, time-local components of gastric emptying may be grouped roughly within “peristaltic pump” or “pressure pump” contributors to transpyloric flow. To better understand this distinction and the analyses that follow, we sketch in Fig. 1 localized antroduodenal pressure changes induced by progressive antral contraction waves superposed on common cavity pressure variations arising from global changes in gastric wall muscle tone. Because transpyloric flow can only occur during periods of positive $P_A - P_D$, phasic changes in positive transpyloric pressure difference localized to the distal antrum are shown in Fig. 1B (solid line, hatched area) rising from a baseline of more gradual changes in $P_A - P_D$ associated with the common cavity component (dashed lines). The phasic changes in transpyloric pressure difference are part of a propagating pressure wave (hatched pressure curves P_1 and P_A)

The costs of publication of this article were defrayed in part by the payment of page charges. The article must therefore be hereby marked “advertisement” in accordance with 18 U.S.C. Section 1734 solely to indicate this fact.

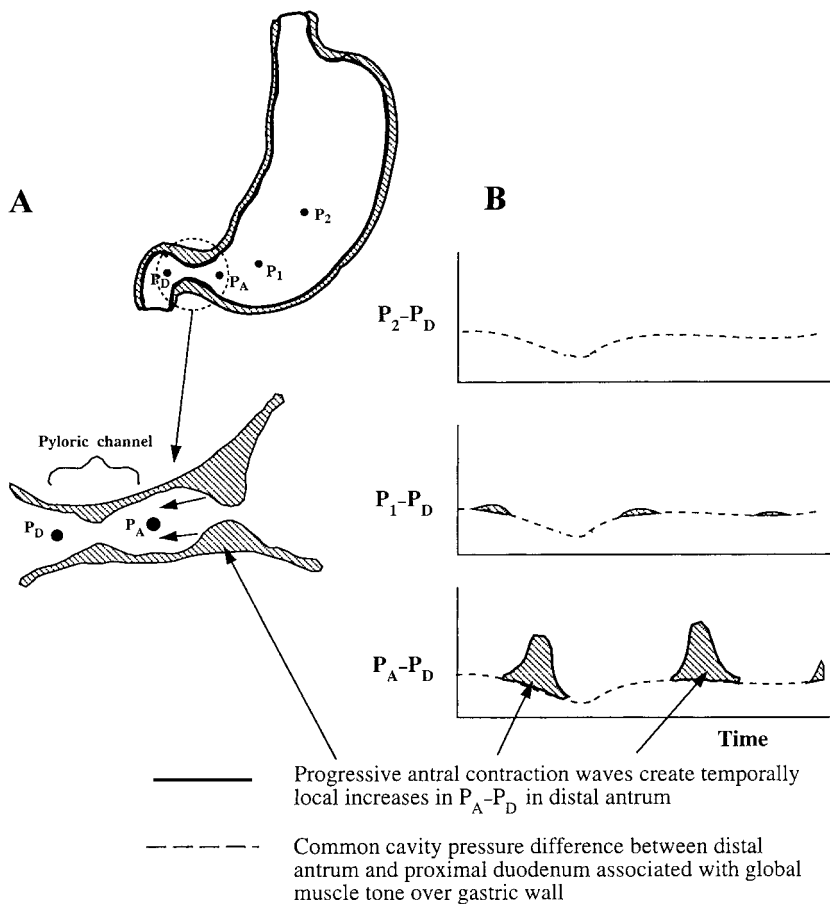


Fig. 1. Schematic of antral pressure activity contributing to "peristaltic pump" and "pressure pump" periods of gastric emptying. A peristaltic pressure wave is induced by an antral contraction wave as it progresses toward pylorus. Time-space local pressure rise (*B*) is slightly distal to advancing geometrical indentation in antral wall (*A*) and rises from a background "common cavity pressure," which itself may vary in time. Whereas progressive indentation in antral geometry is a consequence of a local progressive muscle contraction, common cavity pressure variations may arise from changes in gastric wall tone globally. Transpyloric flow from peristaltic or pressure pump mechanisms requires positive antroduodenal pressure difference ($P_A - P_D$) in presence of an open pylorus.

resulting from localized peristaltic contraction waves (Fig. 1A), whereas the changing baseline pressure in the distal antrum is common to the entire contiguous stomach (dashed pressure curves P_1 , P_2 , and P_A) and may arise from changes in muscle tone anywhere on the gastric wall, including, for example, the fundus.

The peristaltic pump contribution to gastric emptying occurs during the short-duration periods of pressure increase just proximal to the pyloric channel induced by an advancing contraction wave when the pylorus is open. The volume of transpyloric flow during these peristalsis-induced increases in $P_A - P_D$ depends on the magnitude and duration of phasic pressure increase and on the resistance to flow within the pyloric channel. Depending on the diameter of the pyloric channel, flow is directed aborally and orally during phasic increases in antral pressure. If the pylorus is closed, for example, all flow is directed orally and no transpyloric flow occurs. If pyloric resistance is controlled so that the pylorus is fully open as the antral contraction wave advances, on the other hand, optimal contribution to transpyloric flow from antral contractile activity results.

The pressure pump contributor to gastric emptying is associated with flow during periods of relative quiescence in contraction-induced pressure activity in the distal antrum (dashed lines in Fig. 1B). Like the peristaltic pump contribution, the rate of transpyloric flow depends on the

magnitude of the common cavity $P_A - P_D$ and the resistance to flow, as determined by the diameter of the pyloric channel during the quiescent periods.

The relative contributions of peristaltic and pressure pumps to gastric emptying depend on several factors, including the coordination between pyloric opening and phasic pressure excursions in the distal antrum, the degree and duration of opening of the pyloric channel during quiescent periods, and the magnitudes of $P_A - P_D$ during pyloric opening periods. Furthermore, the combination of motor events responsible for emptying depends on physiological responses to the composition of the meal, to gastric volume, and to pharmacological substances that alter gastric or duodenal sensory function (4, 8). In this study we analyze local contributions to emptying delayed by controlled nutrient infusion in the proximal duodenum.

The aim of the present study is to assess the relative contributions to gastric emptying of the pressure and peristaltic pumps in humans during emptying of nonnutrient saline, with the rate of emptying delayed by controlled intraduodenal nutrient infusion. To analyze these primary contributors to gastric emptying, we have concurrently assessed intragastric pressure using high-resolution high-accuracy manometry (6) and antropyloroduodenal anatomy with three-dimensional magnetic resonance (MR) imaging (MRI) (15, 17).

METHODS

Concurrent MRI and high-resolution manometry studies were performed on seven healthy subjects (5 men and 2 women) 23–45 yr of age. All subjects gave written informed consent, and the study was approved by the Ethics Committee of the University Hospital, Zurich. The data were subsequently analyzed using various statistical measures.

Concurrent MRI and High-Resolution Manometry

Subjects fasted overnight before the study. The manometric assembly (4-mm OD) and a second tube (2.5-mm diameter, used for intragastric instillation of saline) were passed into the stomach via an anesthetized nostril. The manometric assembly was positioned across the pylorus by use of transmucosal potential difference (PD_{TM} ; see below). After phase III of the interdigestive migrating motor complex, an intraduodenal infusion commenced. The infusion consisted of a nutrient liquid (equal volumes of 25% dextrose and 10% Intralipid, 1.1 kcal/ml; Kabi-Vitrum, Stockholm, Sweden) delivered at the rate of 2 ml/min (2.1 kcal/min) for the remainder of the study. After 30 min of infusion, the subject was transferred to the MR scanner and positioned lying 30° to the right side to ensure filling of the antrum. An isotonic saline solution (750 or 500 ml) was then infused into the gastric lumen over ~4 min. The saline was marked with 600 μ M Gd-labeled tetraazacyclododecane tetraacetic acid (Laboratoire Guerbet, Aulnay-sous Bois, France) as a contrast agent for MRI. All MRI studies were performed using a Philips Gyroscan ACS-NT 1.5-T whole body scanner.

Figure 2 summarizes the protocol. Within 2–3 min after the stomach was filled, an MR “volume scan” was performed to measure the volume of liquid in the stomach. Two additional volume scans were performed 15 and 30 min later to assess the rate of gastric emptying. Between each pair of volume scans, three “motility scans” were carried out to assess changes in antropyloroduodenal anatomy over time. Manometric pressures were recorded uninterrupted throughout the study with the exception of periodic short periods for recalibration of manometric reference pressure (6). All analysis was carried out for data collected during the 30-min period after gastric filling.

Volume scans. To determine intragastric liquid volume, a Turbo Spinecho scan (repetition time = 576 ms, echo time = 12 ms) with 24 contiguous slices (7.5-mm slice thickness) was acquired over 60 s by a previously established methodology

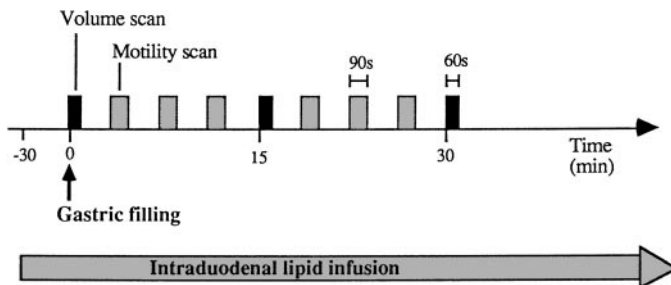


Fig. 2. Schematic of experimental protocol. Gastric emptying was slowed with controlled infusion within proximal duodenum of lipid in water at 2 kcal/min. Gastric volume was measured 3 times at 15-min intervals with magnetic resonance (MR) “volume scans.” Between these intervals, 3 periods of multiplanar “motility scan” were recorded to evaluate time changes in 3-dimensional antral geometry and pyloric location. Data end ~30 min after gastric filling. Pressures on entire manometric assembly were recorded continuously throughout study.

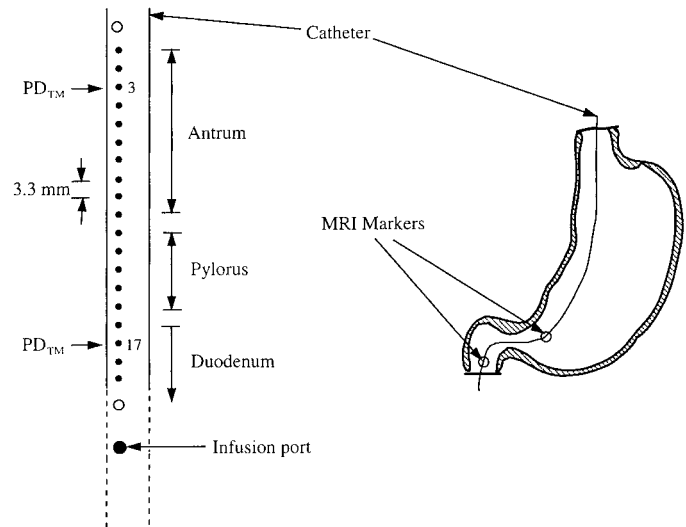


Fig. 3. Schematic of positioning of manometric assembly within antropyloroduodenal region. Pressure was measured at 19 manometric ports spaced at 3.3-mm intervals spanning antropyloroduodenal region. Transmucosal potential difference (PD_{TM}) was measured between ports 3 and 17 for positioning catheter across pylorus. Two metal markers (\circ) were embedded within catheter for identification of catheter position on MR images (MRI).

(16). In-plane pixel resolution was 1.5 mm (256 \times 256 pixels, field of view = 384 mm). To minimize motion artifacts, the scan was divided into four periods of 15 s each, and the subjects were asked to hold their breath during each period. The measured volume necessarily included the ingested liquid and the gastric secretion.

Motility scans. To assess antropyloroduodenal motility and pressure-geometry relationships, rapid multiplanar scans were carried out over multiple 90-s periods. Seven slices were acquired per second by use of a multislice gradient echo planar imaging (EPI) sequence (coronal angulated orientation, EPI factor = 5, echo time = 5 ms, repetition time = 81 ms, flip angle = 20°, matrix size = 128 \times 128 pixels, resolution = 3 mm, field of view = 384 mm, slice thickness = 7 mm). The scan was triggered by a signal from the computer controlling manometric data acquisition to synchronize MRI with manometry.

A perfusion manometry system (Dentsleeve) with optimized electronics (transducer drift <0.1 mmHg/15 min; Sedia, Fribourg, Switzerland) was used to record pressures along a catheter with 21 ports (0.4-mm lumen diameter, 4-mm OD), 19 of which were used for pressure in this study and 1 for intraduodenal nutrient infusion, as illustrated in Fig. 3. The catheter was preflushed with CO₂ to eliminate air bubbles, and water perfusion was limited to 0.08 ml/min. To obtain high spatial resolution through the antropyloroduodenal region, the 19 pressure-recording ports were spaced 3.3 mm apart along a 6-cm segment of the assembly. The 3rd and 17th side holes were perfused with normal saline from separate reservoirs, and PD_{TM} was measured concurrently with manometry to aid the positioning of the catheter across the pylorus. To identify the position of the catheter on MR images, two small stainless steel markers were placed on the catheter at each end of the 19-hole array. The manometric data were recorded for the entire duration of the study at 8 samples/s. Transducer drift was regularly corrected over the study period with use of an underwater reference, and measurement uncertainty was minimized to within 0.5 mmHg (6). The infusion port was ~14 cm below the pylorus.

Data Analysis Methods

The data analyzed were limited to times during which the PD_{TM} readings indicated correct placement of the catheter across the pyloric channel (7). Pressure data were analyzed using several statistical techniques, as described below. In preliminary analysis, it was determined that stable statistics for pressure differences required ~ 4 min of data (2,000 samples collected at 8 samples/s). Thus the analysis was extended beyond the 90-s motility scale periods to include the entire contiguous 30-min period of pressure data.

Statistical analysis of pressure characteristics associated with transpyloric flow required accurate determination of the location of the pylorus along the catheter as a function of time. To this end, the manometric data were interpolated

between ports by use of cubic splines and plotted as contours of constant pressure ("isocontours"), as shown in Fig. 4. During intraduodenal nutrient infusion, a relatively well-defined band of high pressure was observed in the isocontour plots for all subjects, extending ~ 6 –10 mm along the lumen.

Antral, pyloric, and duodenal ports. Figure 4 includes points (with error bars) marking the pyloric location identified from the MR images during motility scan periods, illustrating the correspondence between the high-pressure band and pyloric channel. A separate quantitative analysis (5) confirmed that the high-pressure band corresponded to the anatomic pylorus as determined from the MRI scans. Therefore, because our statistical analyses of pressure used the entire pressure signal, we defined the "pyloric port" as the

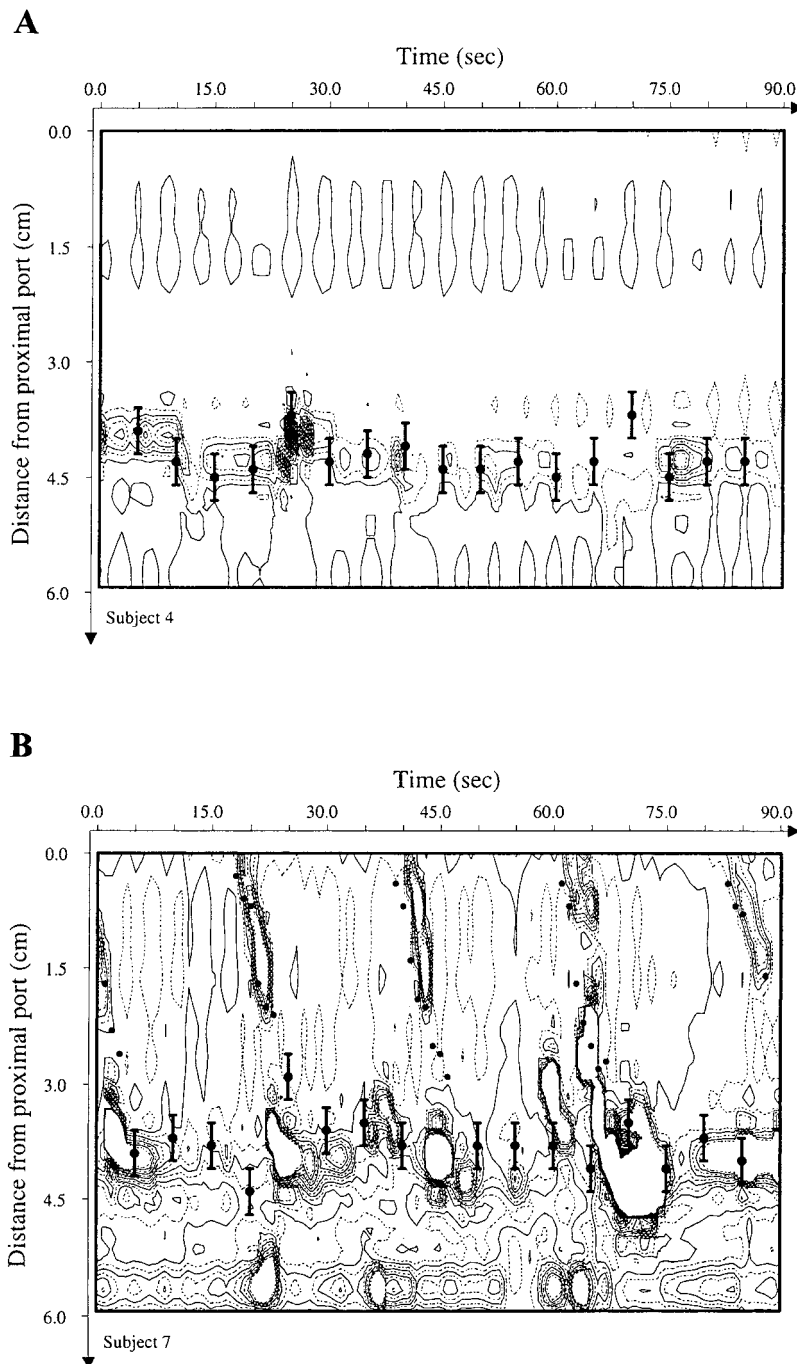


Fig. 4. Isocontour representations of pressure in continuous space-time measured in antro-pyloro-duodenal region with manometric assembly illustrated in Fig. 3. Vertical axis, distance along manometric catheter from most proximal port; horizontal axis, time. Each line is a curve of constant intraluminal pressure, so representation may be read like a "topographic map" of space-time variation in pressure, with "hills" and "valleys" defining structure of intragastric pressure activity within antro-pyloro-duodenal region over time. (All pressures are positive relative to duodenal pressure, and there is no significance in dashed vs. solid isocontours.) Data are displayed during 90-s motility scan periods (Fig. 2), when location of pylorus and antral progression of contraction waves could be independently identified from MR images. These geometrical markers are superposed on pressure isocontours as \bullet : larger \bullet with error bars are MR-measured locations of pylorus; smaller \bullet without error bars are MR-observed contraction waves. In *A* and *B*, a band of high pressure is visible as a concentration of isocontours between ~ 3.0 and 4.5 cm along catheter (ports 11–15). MR-measured pylorus locations coincide with this high-pressure band (5). *A* and *B* are subjects within "low" and "high" antral pressure activity groups, respectively (Fig. 5, Tables 2 and 3); low-activity subject 4 (*A*) emptied at ~ 3 times rate of high-activity subject 7 (*B*). MR-identified peristaltic contraction waves coincide with antral pressure waves in subject 7 (*B*).

manometric port closest to the local maximum in pressure within the high-pressure band. The proximal and distal extremities of the pyloric channel were subsequently identified by the “antral port” and “duodenal port,” defined as the manometric ports 1 cm proximal and 1 cm distal to the pyloric port, respectively. Because the antral, pyloric, and duodenal ports are defined relative to the space-time distribution in antropyloroduodenal pressure, the catheter side holes that define these ports can change with time. Comparison with the MR images confirmed that the ports 1 cm proximal and distal to the pyloric port were within the distal antrum and proximal duodenum, respectively, as also indicated by the pressure isocontours of Fig. 4.

Basal pressures. Antral, pyloric, and duodenal basal pressures (P_A^* , P_P^* , and P_D^*) were defined as the average values of the lowest 5% of the manometric pressures recorded in the antral, pyloric, and duodenal ports, respectively, over the entire data period, with exclusion of recalibration and PD_{FM} misalignment periods. (As a check, P_A^* was also calculated by including all antral channels. The difference between the two approaches was within the imprecision of the measurement.) Because gastric emptying is associated with $P_A - P_D$, all pressures were referenced to P_D^* unless otherwise indicated. Relative P_P^* and P_A^* are catalogued in Table 1.

Level of antral pressure activity. We quantify the differences in levels of phasic and nonphasic pressure activity between subjects in relation to the existence of “high-pressure events” (HPEs), where an HPE is defined as a group of pressure values in any antral channel that exceed a predefined fixed threshold relative to P_A^* . That is, an HPE is a channel-specific period where $P - P_A^*$ exceeds a predefined value $P_{HP} - P_A^*$. Because these periods were used for comparison between subjects, the threshold $P_{HP} - P_A^*$ was set to the same level for all subjects. We discuss below our basis for choosing the particular HPE threshold, $P_{HP} - P_A^* = 5$ mmHg. Antral pressure activity in individual subjects was then quantified using the following statistical measures.

MAXIMUM AREA UNDER THE CURVE. The area under the curve (AUC) was defined in each antral channel as the area under the pressure-time curve during HPE periods. The AUC was calculated with P_A^* as the baseline, and the result was scaled to a total time period of 30 min. To account for intrasubject differences in pressure wave positioning, the antral channel with the maximum AUC (AUC_{max}) was used to distinguish levels of antral pressure activity between subjects.

AVERAGE PRESSURE OF HPES. The “average pressure of HPES” was defined as the average pressure during HPE periods relative to P_A^* in the channel with AUC_{max} .

TOTAL DURATION OF HPES. The “total duration of HPE periods” is the time (in seconds) over which HPEs occurred, scaled to 30 min, in the antral channel with AUC_{max} . Thus

Table 1. Basal pressures and shoulder pressures by use of entire manometric data set

Subject No.	P_A^* , mmHg	P_P^* , mmHg	$P_{SP} - P_A^*$, mmHg
S1	0.4	2.7	3.5
S2	2.8	3.8	3.5
S3	0.0	1.4	4.4
S4	0.4	2.2	3.3
S5	0.6	3.3	4.1
S6	1.1	2.6	4.0
S7	3.7	5.6	4.5

P_A^* and P_P^* , basal antral and pyloric pressures; P_{SP} , shoulder pressure. Pressures are given relative to basal duodenal pressure.

Table 2. Volume of gastric emptying and characteristics of antral HPEs during 30-min periods

Subject No.	VGE, ml	AUC_{max} , mmHg·s	Avg Pressure of HPES, mmHg	Total Duration of HPES, s	Frequency of Propagating HPES, min ⁻¹	Low-Pressure Gap, cm
S1	460	172	5.8	29.6	0.00	
S2	424	1,623	11.7	138.7	1.10	1.4 ± 0.5
S3	408	272	6.4	42.5	0.00	
S4	356	60	8.0	7.5	0.00	
S5	290	1,322	7.5	176.3	1.18	1.3 ± 0.5
S6	160	1,598	9.6	166.5	0.63	3.1 ± 0.3
S7	130	1,660	8.2	202.4	0.96	1.6 ± 0.6

Maximum area under the curve (AUC_{max}) is maximum of $\sum(P_i - P_A^*)\Delta t$ for all samples $(P_i - P_A^*) > 5$ mmHg. Average pressure and total duration of high-pressure events (HPEs) derive from channel with AUC_{max} . Average pressure of HPEs (relative to P_A^*) = $1/N \sum_{i=1}^N (P_i - P_A^*)$ for all samples $(P_i - P_A^*) > 5$ mmHg, where N is the total of samples. Total duration of HPEs = $AUC_{max}/\text{average pressure of HPEs}$. Frequency of propagating HPEs = number of HPEs per minute that propagate at a speed of 2–4 min/s (determined from isocontour plots). Low-pressure gap is an estimate of extent of low-pressure region between antral propagating HPEs and pyloric channel (see Fig. 4B) in “high-pressure activity” group (Fig. 5); values are means ± SD. VGE, volume of gastric emptying.

AUC_{max} = average pressure of HPEs × total duration of HPEs.

These quantifications are discussed further in Table 2.

“Active” periods, “quiescent” periods, and “propagating HPES.” To contrast the relative contributions to gastric emptying of progressive antral pressure events (peristaltic pump) with the intermediate periods of relative quiescence (pressure pump), we first separated antral pressure-time history into subject-specific “high” and “low” pressure periods by using the “shoulder” pressure (P_{SP}), as described in the APPENDIX. The definition of P_{SP} follows from the pressure-time history in the distal antrum in individual subjects, which, as in Fig. 6A, has the structure of spikes of high-pressure activity rising from a bed of low-level pressure fluctuations. As described in detail in the APPENDIX, P_{SP} is an objective measure of pressure, obtained from the “cumulative frequency distribution” (see Fig. 11) that defines the transition between the lower-level pressure fluctuations and the higher, spikier pressure events in the antral pressure port.

As shown in Table 1, relative P_{SP} ($P_{SP} - P_A^*$) was between 3.3 and 4.5 mmHg for all subjects [3.9 ± 0.43 (SD) mmHg]. For this reason, we chose the fixed threshold $P_{HP} - P_A^* = 5$ mmHg, a value just above the highest value of $P_{SP} - P_A^*$, to define HPEs in all subjects.¹ Channel-specific active periods are therefore defined as those periods at a specific channel when $P_A - P_A^*$ exceeds 5 mmHg, whereas channel-specific quiescent periods are the intermediate periods.

PROPAGATING HPES, NONPROPAGATING HPES, AND QUIESCENT PERIODS. We isolated HPEs for all antral channels on the computer and then compared the locations and structure of the extracted HPEs with corresponding space-time structure of pressure in the isocontour plots (Fig. 4). From this comparison, we subjectively separated all channel-specific HPEs into “propagating” groups, which extend across several channels, and “nonpropagating” events. As an objective criterion, we

¹ Interestingly, Stemper and Cooke (18) used the same threshold for counting HPEs in the antrum purely on the basis of subjective observation.

required that all propagating HPEs appear clearly on the isocontour representation as pressure waves across at least three channels with wave speed between 2 and 4 mm/s. Once the propagating subgroupings of HPEs were extracted, the remaining time periods were divided into nonpropagating HPEs and quiescent periods. In this way, the pressure-time history in the antral ports of all subjects was subdivided into propagating HPEs, nonpropagating HPEs, and quiescent periods.

Window means. The time mean of a quantity X (where X could be, e.g., pressure or pressure gradient) was defined over specified periods, excluding periods where the PD_{TM} readings indicated incorrect placement of the catheter across the pyloric channel. To assess the variation of basal and mean pressure with time, we divided the data period into shorter time intervals, or "windows," and computed the mean and basal pressures within each window. The minimum time interval had to be sufficiently long to contain enough sample for stable statistics. Tests suggested that ≥ 2 min of sample (1,000 at 8 samples/s) were required for stable pressure statistics (4 min for pressure difference). Thus the total time interval was separated into three time windows with $\geq 2,000$ pressure samples in each window. Basal pressure and time averages were computed for each time window.

The pressure gradient ($\Delta P/L_p$) across the pyloric channel was estimated as $(P_A - P_D)/L_p$, where L_p is the distance between the antral and duodenal ports (2 cm).

RESULTS

Emptying vs. High-Pressure Activity in the Antrum

In Table 2, subjects are numbered from the highest to the lowest gastric volumes emptied during the first 30 min after gastric filling. The volume of gastric emptying (VGE) differed widely among subjects, and the average pressure during HPEs varied from 5.7 to 12.0 mmHg above P_A^* with no correlation with volume emptied. However, AUC_{max} varied from 60 to 1,660 mmHg·s in such a way that all subjects could be clearly separated into high and low antral pressure activity groups (Fig. 5), where AUC_{max} was 9–10 times lower in the low-pressure activity group (subjects 1, 3, and 4) than in the high-pressure activity group (subjects 2, 5, 6, and 7). Correspondingly, the total durations of HPEs were significantly higher in the high antral pressure activity group (Table 2). As indicated in Table 3, the low-activity subjects displayed no propagating HPEs, and a significantly higher percentage of time was occupied by quiescent periods [98 ± 2.8 vs. $76 \pm 9.4\%$ (SD)] in the low-activity group. Nevertheless, Fig. 5 indicates that the volume of liquid emptied was higher, on average, in the low-pressure activity group (251 and 408 ml in the high- and low-activity groups, respectively). The correlation coefficient between VGE and AUC_{max} was -0.65 , although there are too few samples in each group to verify statistical significance. Thus statistically there was no significant difference in emptying between the two groups of subjects that differed by an order of magnitude in level of antral pressure activity!

Figure 4 compares the space-time pressure history during a 90-s motility scan period in members of

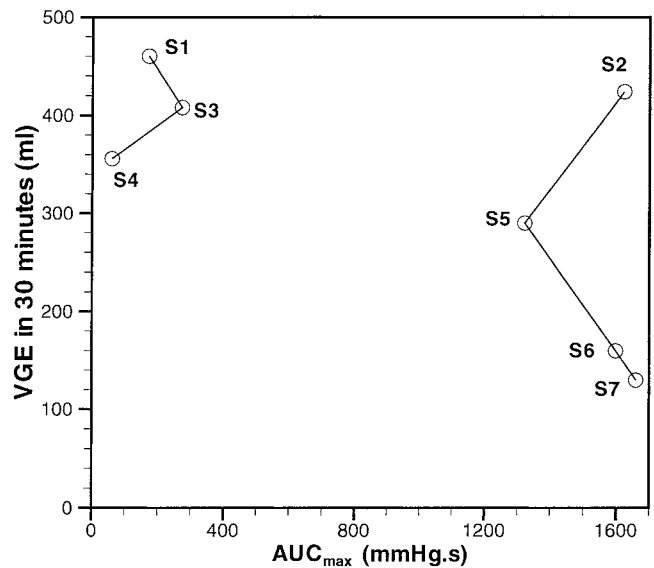


Fig. 5. Level of antral pressure activity, as defined by maximum area under curve (AUC_{max}), plotted against volume of gastric emptying (VGE) over a 30-min period between 1st and 3rd volume scans (Fig. 2). Seven subjects organized neatly into "high-pressure activity" [subjects 2, 5, 6, and 7 (S2, S5, S6, and S7)] and "low-pressure activity" [subjects 1, 3, and 4 (S1, S3, and S4)] groups. (Figure 4 shows representative space-time pressure structure over 90-s periods for a subject in each group.) Although average VGE in high-activity group (251 ml) was lower than average VGE in low-activity group (408 ml), difference was not statistically significant.

the low- and high-activity groups. Whereas Fig. 4A shows relatively little high-pressure activity proximal to the pyloric channel, Fig. 4B shows clear high-amplitude peristaltic pressure wave activity. These time-space pressure characteristics were typical of the two groups.

Figure 4B also shows the termination of the antral pressure waves ~ 1 cm preceding the pyloric channel, creating a gap of low pressure. The length of this "low-pressure gap" is tabulated in Table 2 for the four "high-activity" subjects. Subject 6 differed from the other three high-activity subjects (subjects 2, 5, and 7), in that the low-pressure gap was over twice as wide (3.1 cm for subject 6 vs. 1.4, 1.3, and 1.6 cm for subjects 2, 5, and 7). This difference affects subsequent statistics (see below).

Table 3. Percentage of time occupied by quiescent periods, nonpropagating HPEs, and propagating HPEs averaged over antral channels

Subject No.	QP	NPHPE	PHPE
S1	98.8	1.2	0
S2	73.4	3.3	23.3
S3	95.5	4.5	0
S4	99.8	0.2	0
S5	75.5	3.4	21.1
S6	89.8	3.1	7.1
S7	63.5	5.0	31.5

QP, quiescent period; NPHPE, nonpropagating HPE; PHPE, propagating HPE.

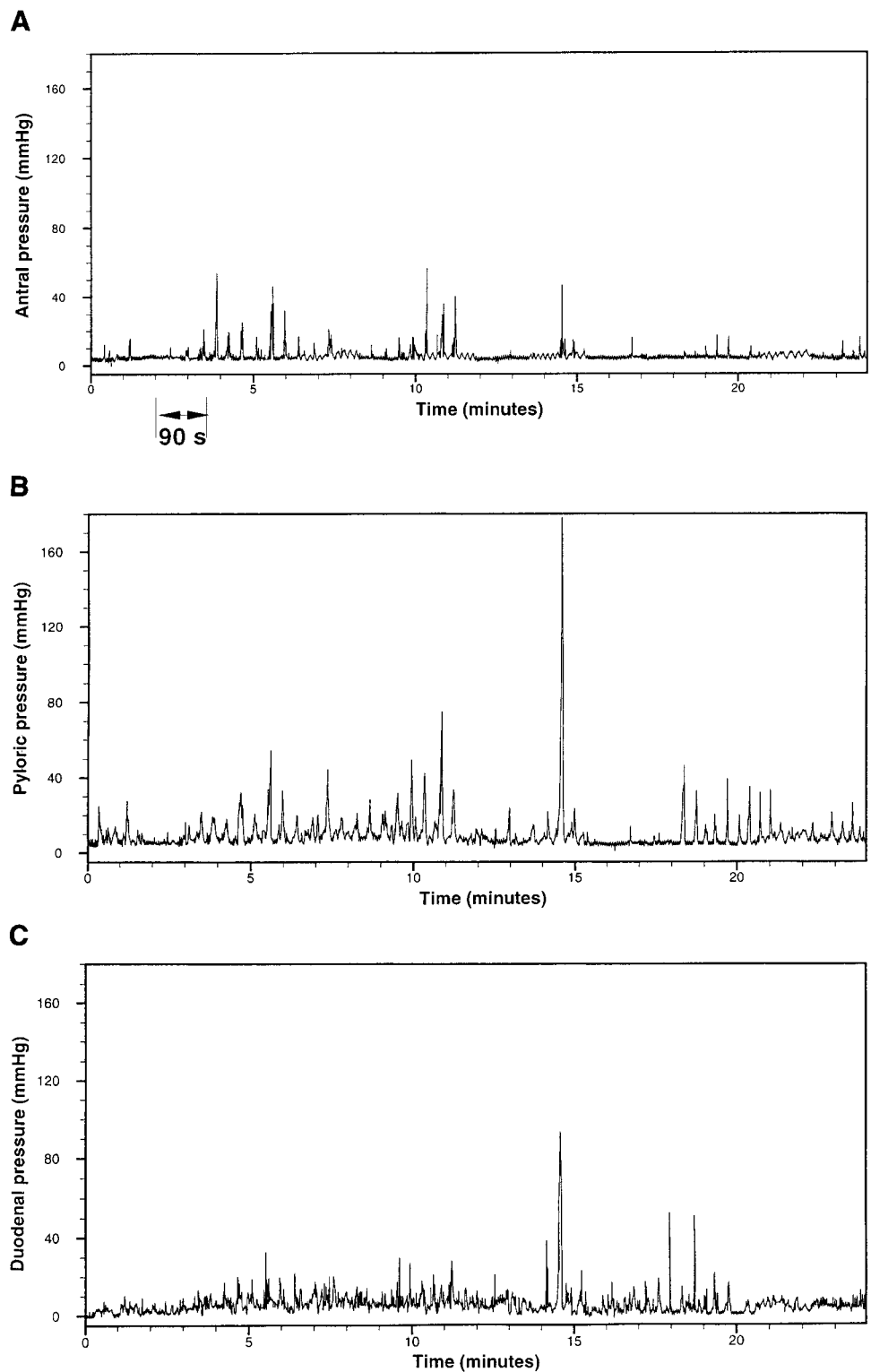


Fig. 6. Variations in antral (A), pyloric (B), and duodenal (C) pressures over ~30-min periods measured from antral, pyloric, and duodenal ports, respectively (see METHODS) for *subject 2* in high antral pressure activity group (Fig. 5). All pressures are shown relative to basal pressure in duodenal port (P_D^*). Basic structure in antral pressure variation is one of intermittent high-pressure spikes rising from a bed of low-level pressure fluctuations. In APPENDIX, a pressure threshold P_{SP} is defined that objectively separates spikier antral pressure events from lower-level fluctuations. Note different perspective obtained from single-channel manometry over extended periods of time compared with space-time structure over 90-s periods shown in Fig. 4 encompassing only a few antral peristaltic events. Whereas Fig. 4 shows structure of space-time pressure variation throughout antro-pyloro-duodenal region, longer-time intermittent pressure rising from lower-level pressure fluctuations, each of which has potential to contribute to gastric emptying, is emphasized here.

Basal and Mean Pressures and Pressure Gradient

Figure 6 shows a representative example of time history of antral, pyloric, and duodenal pressures measured from the antral, pyloric, and duodenal ports over ~30 min for high-activity *subject 2*. All pressures are referenced to P_D^* . Particularly evident in antral and pyloric pressure are intermittent spikes in pressure

overlying low-level pressure fluctuations. Also evident is the overall higher baseline pressure in the antrum than in the duodenum (Table 1).

To assess the overall changes in background pressure during gastric emptying, we plot in Fig. 7 average antral and pyloric port pressures measured within the quiescent periods in each of three time windows spanning the ~30-min data periods (see METHODS). Whereas

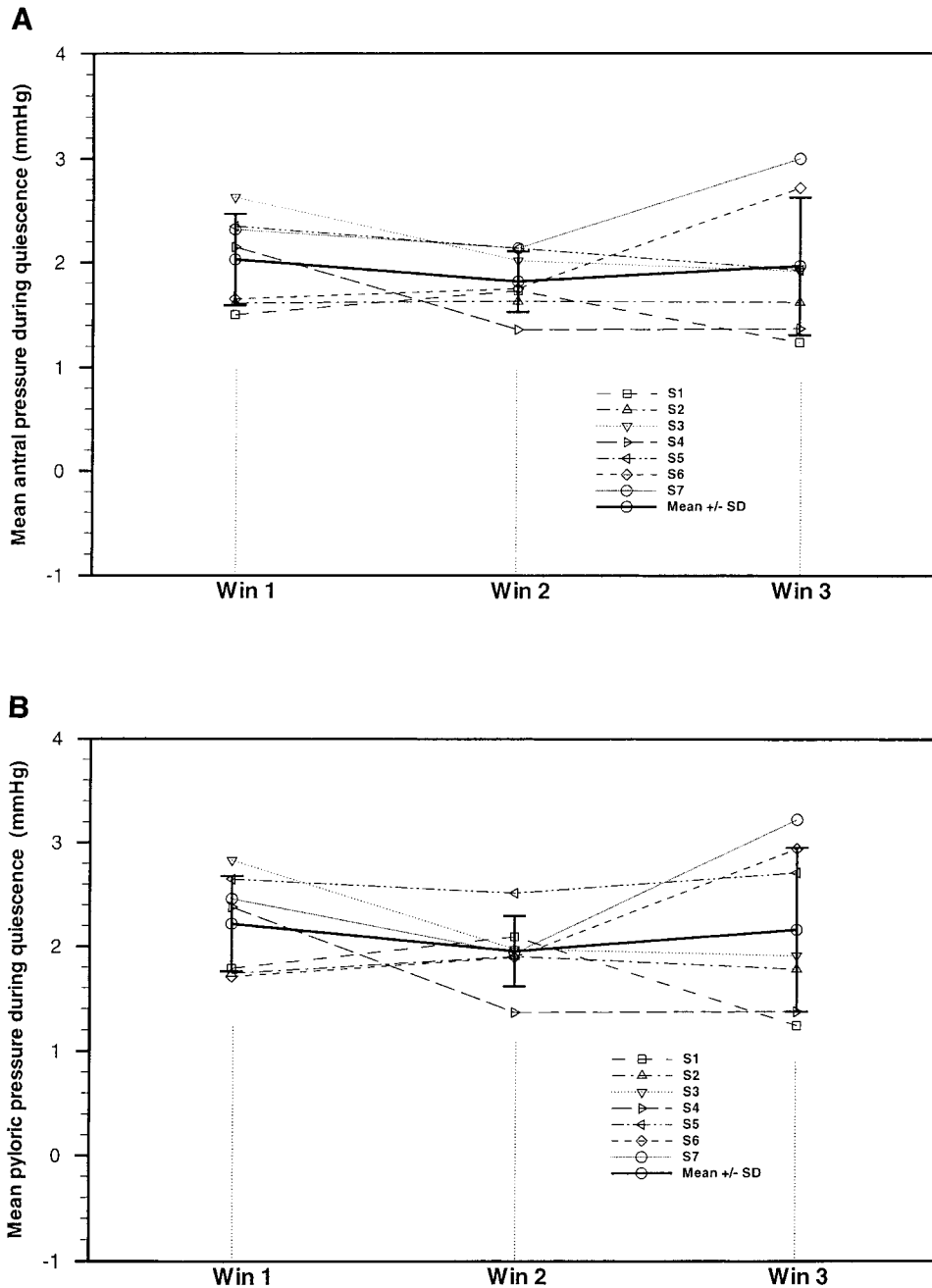


Fig. 7. Average pressure statistics from antral (A) and pyloric (B) ports over 3 time windows (Win 1, Win 2, and Win 3) of ~10 min each during "quiescent periods" of pressure variation in respective ports. In antral channel, "quiescence" is defined as periods when pressure was below HPE threshold ($P_{HP} - P_A^* = 5$ mmHg, where P_A^* is basal antral pressure). In pyloric port, quiescence is defined as periods when pressure was below P_{SP} obtained from cumulative frequency distribution (CFD) of pyloric pressure (see APPENDIX). All pressure statistics are given relative to P_A^* . Dark solid curves, averages over 7 subjects during each windowed period; error bars, SD.

the quiescent period was defined in the antral port by using the 5-mmHg threshold described in METHODS, in the pyloric port the quiescent periods of pyloric pressure were defined using the P_{SP} in that port (see METHODS and APPENDIX).

In Fig. 7, pressures are referenced to P_A^* (Table 1). Figure 7 indicates that the average pressures during quiescence in the antral and pyloric channels are on the order of 2 mmHg above P_A^* . More importantly, there was no significant change in average antral and pyloric pressure during the periods of quiescence during the 30-min periods of gastric emptying ($P \approx 0.6$).

We also found statistically insignificant changes in windowed mean basal pressure over the 30-min period averaged over the seven subjects (not shown). We

found, by examining in detail the changes in P_A^* and quiescent pressure from the first to the third window, that those subjects with a small increase or decrease in average pressure during periods of quiescence also had a corresponding small increase or decrease in basal pressure in the antrum is correlated with P_A^* .

The mean pressure gradient across the pyloric channel from the antral to the duodenal port averaged over all subjects was 0.3 ± 0.2 (SD) mmHg/cm.

Antral-Pyloric Pressure Relationships

In Fig. 4B, the periods when progressive antral pressure waves exist appear to be also periods of high

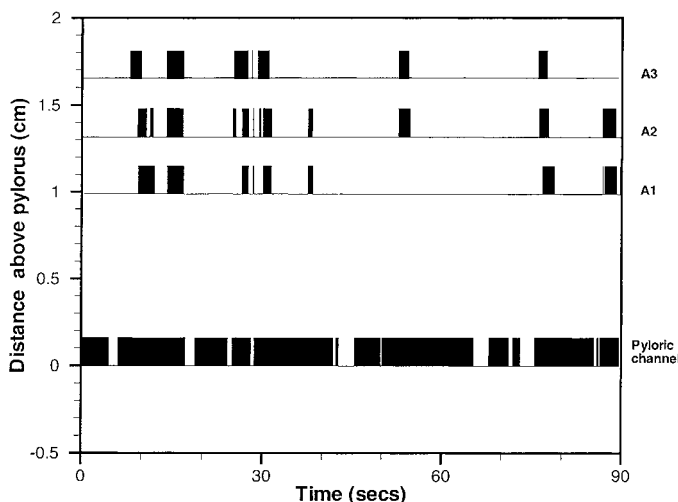


Fig. 8. "Active" and "quiescent" periods in pyloric channel and in 3 antral channels over a 90-s time window (different from Fig. 4B). Filled bars, active periods; periods between filled bars, quiescent periods. In pyloric channel, active periods are those in which antral pressure exceeds 5 mmHg relative to P_A^* . In pyloric channel, active periods are those where pressure exceeds P_{SP} defined for pyloric channel from CFD (see APPENDIX). Progressive antral pressure waves occur during periods when resistance to transpyloric flow is high, and quiescent periods in pyloric channel tend to occur during quiescent periods in antral pressure.

pyloric pressure. This subjective observation is made clearer in Fig. 8, where the active and quiescent periods are shown in the pyloric channel and in the first three antral channels (Fig. 7). In the pyloric port the quiescent periods are those with the least pyloric resistance and, therefore, are the most likely to allow transpyloric flow. We observe that during this 90-s period the pyloric quiescent periods occur during periods of quiescence also in the antral channels and that the resistance to transpyloric flow appears to be highest during antral pressure wave periods.

To determine whether this subjective observation is a general one, we search for a statistical relationship between antral peristaltic wave activity and pyloric resistance (measured by pressure) in the four high-activity subjects. In Fig. 9 we show, for each subject, pairs of frequency distributions of pressures in the pylorus during periods of propagating HPEs in the antrum and periods of antral quiescence, designated as described in METHODS. *Subjects 2, 5, and 7* display similar characteristics: at the lowest pyloric pressures, within a few mmHg from P_p^* when the resistance to transpyloric flow is at a minimum, the fraction of samples is very much lower during propagating antral HPEs than during quiescent periods in the antrum. This drop in the fraction of pressure samples in the range P_p^* to $P_p^* + 4$ mmHg is roughly a factor of 2 and is statistically significant ($P = 0.028$). Thus the probability of transpyloric flow for these three subjects is significantly higher during antral quiescent periods than during antral propagating pressure waves.

The same trend is not observed with *subject 6*. This difference is a direct reflection of the difference in extent of the low-pressure gap that precedes the pyloric

channel (Fig. 4B). Because the low-pressure gap is over twice as wide in *subject 6* as in *subjects 2, 5, and 7* (Table 2), the antral peristaltic pressure waves progress to only within ~ 3 cm of the pyloric channel before terminating. As a consequence, these distant peristaltic pressure waves had little influence on pyloric pressure variation for this subject.

The relationship between pyloric resistance and antral pressure activity is analyzed further in Fig. 10, where the level of pyloric resistance is correlated with the advancement of antral contraction waves. Specifically, average pyloric pressure for the periods when propagating HPEs pass each antral pressure port is plotted in Fig. 10 as a function of the antral port number. The antral ports are numbered A1–A8 from the most distal to the most proximal, each port separated by 3.3 mm beginning with *port A1*, which is 1 cm proximal to the pyloric port. The average pressure in the pyloric port is plotted relative to P_D^* . Figure 10 shows that pyloric resistance increases as antral pressure waves move closer to the pylorus. The increase in pyloric pressure with decreasing distance from the pylorus is significant in *subjects 2, 5, and 7* ($P = 0.038$). Consistent with Table 2, the advancing pressure waves in *subject 6* terminate much more proximally than in *subjects 2, 5, and 7*. Figure 10 suggests that the pyloric response to antral pressure waves may not begin until the antral waves are 2–3 cm above the pylorus and that the peristaltic pressure waves in *subject 6* terminate before a pyloric response is triggered.

DISCUSSION

Gastric emptying is analyzed in this study as a series of local transpyloric flow events that integrate to produce a reduction in gastric volume of 130–460 ml over a 30-min period (Table 2). Time-local transpyloric flow events can be roughly classified in two groups: flow associated with local increases in $P_A - P_D$ due to antrally propagating pressure waves and flow associated with a common cavity pressure difference between the distal antrum and the proximal duodenum in periods of quiescence between antral HPEs. The first class of flow events is associated mechanically with a peristaltic pump mechanism of flow and the second class with a pressure pump mechanism of transpyloric flow. Whereas propagating pressure waves originate from corresponding localized propagating contraction waves, as illustrated in Fig. 1, common cavity pressure changes can also arise from global tonic sources dispersed anywhere over the gastric wall.

On the other hand, flow can only occur in the presence of an open pylorus. The sensitivity of flow to the degree of pyloric opening is evident through a relevant fluid physics approximation for viscous flow through constrictions (2, 11, 12), which indicates that the rate of transpyloric flow at any instance in time is proportional to $(P_A - P_D)/R$, where R is pyloric resistance at that time. R is given by μ/D^4 , where D is the average diameter of the pyloric channel and μ is the gastric fluid viscosity. Because the R is proportional to $1/D^4$, there is great sensitivity between the rate of

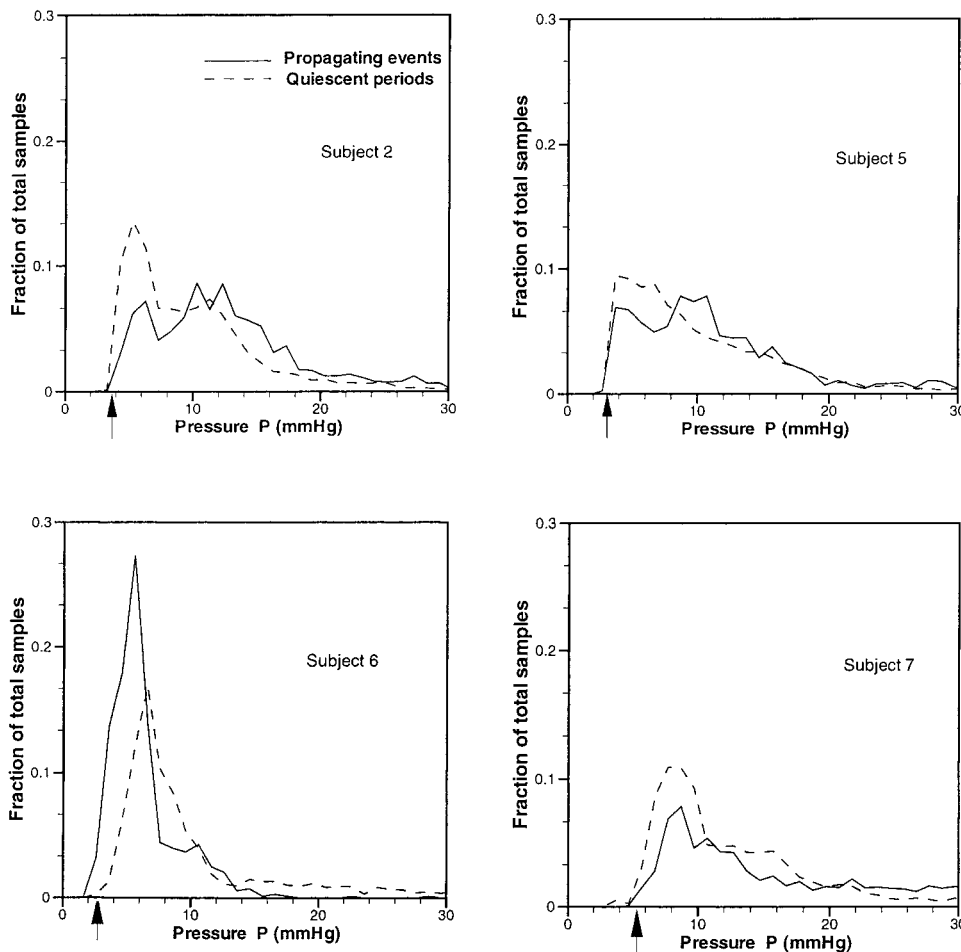


Fig. 9. Fraction of total samples below a variable pyloric pressure (P , frequency distribution) conditioned on periods of time where propagating HPEs exist in antrum and on periods of quiescence in antral pressure activity for 4 subjects in high-activity group (Fig. 5). Pyloric pressures are given relative to P_b^* . Vertical arrows, pyloric basal pressure (P_b^* , Table 1). In *subjects 2, 5, and 7*, fraction of samples between P_b^* and $P_b^* + 4$ mmHg drops significantly during periods of antral propagating pressure waves. Such a drop does not occur in *subject 6* because of exceptionally large “low-pressure gap” between end of antral contraction waves and pyloric channel (Table 2).

transpyloric flow and pyloric diameter. Consequently, our evaluations of peristaltic vs. pressure pump contributions to gastric emptying center on correlations between antroduodenal pressure history and changes in R measured indirectly through pyloric pressure.

Gastric emptying follows from the relationships between the pressure forces, which move the gastric contents against frictional resistance, and the gastric wall motions and muscle tone, which generate those pressure forces. Measurement of pressure-geometry relationships associated with emptying requires concurrent manometry with imaging in the antropyloroduodenal region, where emptying is controlled and where resolution requirements are most severe. We combined three-dimensional MRI and high-resolution manometry to monitor pressure-geometry motor events in the antropyloroduodenal regions of seven subjects while simultaneously measuring changes in gastric volume over 15-min intervals during emptying of a nonnutrient liquid with intraduodenal nutrient infusion at 2 kcal/min.

The seven subjects differed in the nature of high-pressure activity in the antrum: three subjects displayed little high-pressure activity, and four subjects exhibited consistent propagating high-pressure antral events. Consequently, the seven subjects separated neatly into “high antral activity” and “low antral activity”

groups quantified by AUC (AUC_{max}), frequency, and total duration of HPEs. Interestingly, whereas AUC_{max} was 10 times higher in the high-activity group, there was no significant difference in the rate of gastric emptying. Indeed, the correlation between the rate of emptying and antral pressure activity was -0.65 , suggesting a tendency for a lower rate of emptying with higher levels of antral contractile activity (Table 2, Fig. 6). This observation was the first indication that antral pressure wave activity may not play the dominant role in slowed gastric emptying.

A second indication was given by Fig. 7, which shows that average antral pressure during quiescent periods of antral activity (also P_A^*) remained unchanged during reductions in gastric volume from 130 to 460 ml over 30 min. If the stomach wall were a purely elastic structure, emptying would imply decreasing elastic wall tension and decreasing intragastric pressure until the internal and external pressures equalize. Figure 7, on the other hand, suggests that active muscle wall tone increased, on average, during gastric emptying. Furthermore, whereas active tone apparently increased with decreasing gastric volume in all subjects, there was much variability in antral high-pressure activity among subjects (Table 2, Fig. 5), suggesting that increases in active wall tone are independent of contractile activity within the antrum. Because transpyloric flow is driven

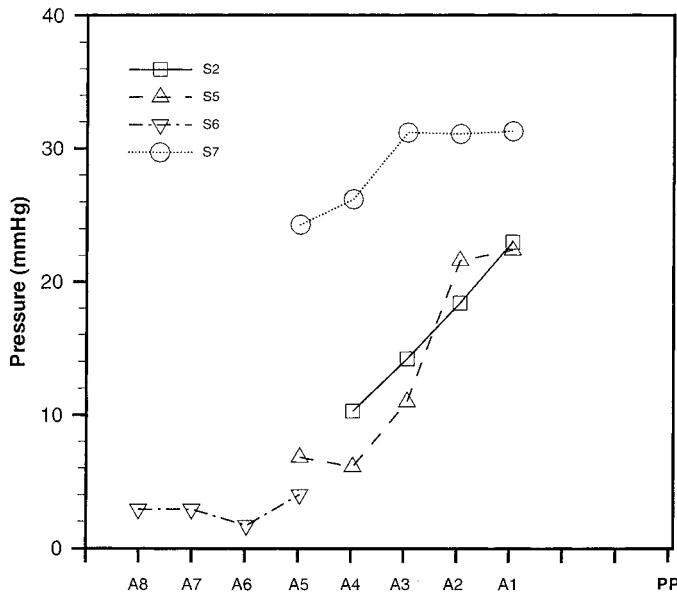


Fig. 10. Average pressure at pyloric port conditioned on existence of propagating HPEs at different antral channels proximal to pyloric port. A1–A8, locations of antral channels beginning with “antral port” (1 cm above pyloric port) and progressing proximally with each adjacent antral channel (each separated by 3.3 mm). Left axis, average pressure in pyloric port (relative to P_D^*) during periods when propagating HPEs could be found at various antral ports, with A8 being most distant port and A1 port closest to pylorus. Pyloric pressure has a significant tendency to be higher when pressure wave is closer to pylorus.

by a pressure drop across an open pylorus, the maintenance of constant common cavity pressure levels in the presence of major reductions in gastric volume suggests a physiological response to the decrease in gastric volume so as to maintain transpyloric flow in the absence of antral contraction-wave activity during periods of pyloric opening.

Furthermore, we found also that average pyloric pressure during quiescent periods in the pyloric channel is insensitive to changes in gastric volume (Fig. 7B). Tougas et al. (19) found that increases and decreases in the pyloric pressure on the order of 2 mmHg relative to P_A^* appeared to be correlated with pyloric closure and opening, respectively. Thus a significant decrease in the average pyloric pressure during quiescence over the 30-min period might have suggested that gastric emptying was maintained by a continual increase in the duration of pyloric opening. By contrast, the insensitivity of pyloric and antral pressures during quiescent periods to reductions in gastric volume suggests a significant role for common cavity pressure difference in gastric emptying.

Further evidence that the pressure pump may be an important contributor to gastric emptying during intraduodenal nutrient infusion is given in Table 3, where we find that antral pressure activity in the three low-activity subjects (*subjects 1, 3, and 4*) is almost entirely quiescent with no evidence of antral propagating pressure waves. Surprisingly, there was no statistically significant difference in the average rate of gastric emptying between these three subjects and the four

subjects that displayed high levels of gastric emptying (Fig. 5), suggesting that the emptying was primarily from common cavity pressure difference in the presence of an open pylorus and that antral peristaltic activity has the potential to impede emptying. For this to be the case, transpyloric flow must be slowed during antral peristaltic pressure events. This conclusion follows from Figs. 8–10.

Figure 8 suggests that the presence of antral contraction waves is correlated with high pyloric resistance; statistical evidence supporting this conjecture is given in Figs. 9 and 10. For antral peristaltic contractions to contribute significantly to gastric emptying, increases in peristalsis-induced pressure in the distal antrum should be correlated with low pyloric resistance. We find just the opposite, however. Figure 9 shows that pyloric pressure was significantly higher during antral propagating pressure events than during quiescent periods of antral pressure activity, implying that the pylorus has a higher probability to be closed during peristaltic activity in the antrum than during the quiescent periods between HPEs.

More significantly, Fig. 10 suggests an interaction between pyloric resistance and the relative location of advancing peristaltic pressure waves. Within a zone of influence, it appears that the closer the peristaltic wave to the pylorus, the greater the probability of the pylorus to be closed. The peristaltic waves in one high-activity subject (*subject 6*) appear to terminate outside this zone of influence, so pyloric resistance is not influenced by the advancing pressure wave (Fig. 10). Because $P_A - P_D$ is unaffected by the propagating pressure waves in this subject, peristalsis does not contribute significantly to emptying.

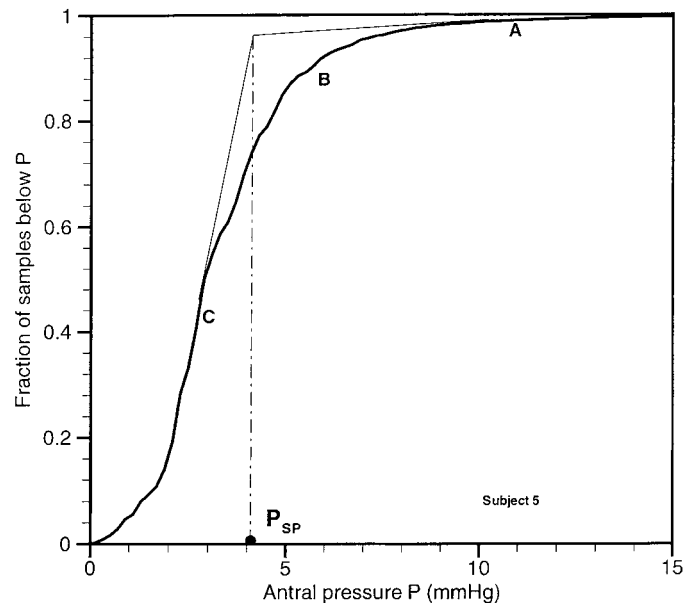


Fig. 11. CFD from *subject 5*. CFD is defined as fraction of samples below a variable threshold P , referenced to P_A^* , and was used to define a subject-dependent P_{SP} that demarcates transition between lower-level fluctuations and higher-level spikes in antral pressure-time history (see Fig. 6A).

We are led to hypothesize, therefore, that when gastric emptying is sufficiently delayed by nutrient stimulation of the duodenum, antral peristaltic wave activity interacts with pyloric opening to increase pyloric resistance and impede transpyloric flow during local periods when the peristaltic events have the highest potential to contribute to gastric emptying. Furthermore, we hypothesize that this interaction occurs within a zone of influence that appears to be on the order of 2–3 cm from the pylorus.

The overall conclusion that gastric emptying of nutrient liquids occurs primarily during periods of quiescence in antral pressure activity and, by implication, in antral contractile activity is consistent with a subjective observation made by Brown et al. (Ref. 3, p. 435) in their visual examinations of ultrasound images during emptying of chicken broth and beans from the human stomach. More quantitative observation from ultrasound images during emptying by Pallotta et al. (14) concludes, consistent with this study, that transpyloric flow of a nutrient liquid meal occurred primarily during periods “not associated with occlusive antral or duodenal proximal contraction.” However, they go on to suggest, inconsistent with Fig. 10, no coordination between pyloric closure and antral contraction. Clearly, additional study of the fundamental mechanics and underlying neurophysiology is warranted.

In summary, we conclude from this study that, during gastric emptying of liquids slowed by controlled duodenal nutrient infusion at 2 kcal/min, gastric emptying was dominated by pressure pump mechanics resulting from common cavity pressure differences between the distal antrum and the proximal duodenum. Whereas antral peristalsis was common in four of the seven subjects, the peristaltic pump mechanism of transport across the pyloric channel contributed only minimally to gastric emptying because of relatively refined physiological coordination between antral peristalsis and pyloric resistance. Indeed, these results suggest that the delay in gastric emptying induced by nutrient stimulation of the duodenum follows from a coordinated response in which antral contractile activity increases together with increases in periods of high pyloric resistance and that this coupling may be controlled by a physiological response within a zone of influence extending proximally from the pylorus.

It should be stressed that the protocol analyzed here is specific to gastric emptying slowed by controlled intraduodenal infusion of nutrients at 2 kcal/min. It would be of great interest to extend the analysis to a wider range of gastric emptying states and larger samples within the high- and low-activity groups.

APPENDIX

Cumulative frequency distribution and P_{SP} . The antral port cumulative frequency distribution (CFD) of pressure is shown in Fig. 11 for *subject 5* (with pressure characteristics similar to Fig. 6A). The CFD is defined as the fraction of pressure samples in the antral port below a variable pressure P plotted against P relative to P_{λ} . Clearly, the CFD must equal 0 at P below the lowest pressure (approximately P_{λ}), and the CFD must approach 1 as P approaches the highest pressure in the

data set. The shape of the curve between 0 and 1, however, is due to the structure of the signal. Figure 6A displays intermittent spikes in pressure rising from a low-level bed of pressure fluctuations. Consequently, as the threshold P increases from the basal pressure ($P = 0$), it encounters the highest density of pressure samples, and the CFD increases rapidly (curve portion C in Fig. 11). However, the density of intermittent spikes is much lower, so that as P increases from the lower-level fluctuations to the higher-level intermittent spikes, the rate of increase in the CFD slows dramatically (portion B in Fig. 11) and the CFD approaches a plateau (portion A in Fig. 11) at the highest-level spikes in pressure.

The pressures in curve portion B represent the transition between HPEs and periods of relative quiescence. To objectively quantify a single pressure value that defines this transition, we identify the intersection pressure between two straight lines that are fit to curve segments A and C of the CFD, as shown in Fig. 11. We term this transitional pressure P_{SP} .

We thank Dr. Karen Quigley for help with statistical analysis of the data.

This study was supported by the Janssen Research Foundation, Swiss National Science Foundation Grant 32-45982.95, and Janssen-Cilag.

This study was reported in abstract form (10); related abstracts are Refs. 5 and 9.

Address for reprint requests and other correspondence: J. G. Brasseur, 205 Reber Bldg., Dept. of Mechanical Engineering, Pennsylvania State University, University Park, PA 16802 (E-mail: brasseur@jazz.me.psu.edu).

Received 10 February 1999; accepted in final form 18 November 1999.

REFERENCES

1. Anvari M, Dent J, and Jamieson GG. Mechanics of pulsatile transpyloric flow in the pig. *J Physiol (Lond)* 488: 193–202, 1995.
2. Brasseur JG and Dodds WJ. Interpretation of intraluminal manometric measurements in terms of swallowing mechanics. *Dysphagia* 6: 100–119, 1991.
3. Brown BP, Schulze-Delrieu K, Schrier JE, and Abu-Yousef MM. The configuration of the human gastroduodenal junction in the separate emptying of liquids and solids. *Gastroenterology* 105: 433–440, 1993.
4. Camilleri M, Malagelada J-R, Brown ML, Becker G, and Zingsmeister AR. Relation between antral motility and gastric emptying of solids and liquids in humans. *Am J Physiol Gastrointest Liver Physiol* 249: G580–G585, 1985.
5. Faas H, Hebbard G, Kunz P, Brasseur JG, Schwizer W, Indireskumar K, Feinle C, Dent J, Fried M, and Boesiger P. Erythromycin-induced alterations to antro-pyloro-duodenal motility studied by combined manometry and MRI (Abstract). *Gastroenterology* 114: A750, 1998.
6. Hebbard GS, Feinle C, Kunz P, Faas H, Boesiger P, Fried M, and Schwizer W. Technical aspects of high-resolution perfusion manometry—an underwater zero improves accuracy of measurement of catheter offset and transducer drift (Abstract). *Gastroenterology* 112: A744, 1997.
7. Hedde R, Dent J, Touli J, and Read NW. Topography and measurement of pyloric pressure waves and tone in humans. *Am J Physiol Gastrointest Liver Physiol* 255: G490–G497, 1988.
8. Horowitz M, Dent J, Fraser R, Sun W, and Hebbard G. Role and integration of mechanisms controlling gastric emptying. *Dig Dis Sci* 39, Suppl: 7S–13S, 1994.
9. Indireskumar K, Brasseur JG, Faas H, Hebbard GS, Kunz P, Dent J, Boesinger P, Feinle C, Fried M, Li M, and Schwizer W. Variables affecting the difference in rate of gastric emptying among subjects (Abstract). *Gastroenterology* 114: A750, 1998.
10. Indireskumar K, Faas H, Brasseur JG, Hebbard GS, Kunz P, Dent J, Boesinger P, Feinle C, Fried M, Li M, and

- Schwizer W.** Relative contribution of "pressure pump" and "peristaltic pump" to gastric emptying (Abstract). *Gastroenterology* 114: A750, 1998.
11. **Kahrilas PJ, Lin S, Spiess AE, Brasseur JG, Joehl RJ, and Manka M.** The impact of fundoplication on bolus transit across the gastroesophageal junction. *Am J Physiol Gastrointest Liver Physiol* 275: G1386–G1393, 1998.
 12. **Li M, Brasseur JG, and Dodds WJ.** Analysis of normal and abnormal esophageal transport using computer simulations. *Am J Physiol Gastrointest Liver Physiol* 266: G525–G543, 1994.
 13. **Malbert CH, Mathis C, and Laplace JP.** Vagal control of pyloric resistance. *Am J Physiol Gastrointest Liver Physiol* 269: G558–G569, 1995.
 14. **Pallotta N, Cicala M, Frandina C, and Carazziari E.** Antropyloric contractile patterns and transpyloric flow after meal ingestion in humans. *Am J Gastroenterol* 93: 2513–2522, 1998.
 15. **Schwizer W, Fraser R, Borovicka J, Asal K, Crelier G, Boesiger P, Convers JJ, Blum AL, and Fried M.** Effect of a calorie load on proximal and distal gastric motility measured by magnetic resonance imaging in humans (Abstract). *Gastroenterology* 104: A579, 1993.
 16. **Schwizer W, Fraser R, Borovicka J, Asal K, Crelier G, Kunz P, Boesiger P, and Fried M.** Measurement of proximal and distal gastric motility with magnetic resonance imaging. *Am J Physiol Gastrointest Liver Physiol* 271: G217–G222, 1996.
 17. **Schwizer W, Maecke H, and Fried M.** Measurement of gastric emptying by magnetic resonance imaging in humans. *Gastroenterology* 103: 369–376, 1992.
 18. **Stemper TJ and Cooke AR.** Gastric emptying and its relation to antral contractile activity. *Gastroenterology* 69: 649–653, 1975.
 19. **Tougas G, Anvari M, Dent J, Somers S, Richards D, and Stevenson GW.** Relation of pyloric motility to pyloric opening and closing in healthy subjects. *Gut* 33: 466–471, 1992.
 20. **Treacy PJ, Jamieson GG, and Dent J.** The importance of the pylorus as a regulator of solid and liquid emptying from the stomach. *J Gastroenterol Hepatol* 10: 639–645, 1995.
 21. **Treacy PJ, Jamieson GG, and Dent J.** Pyloric motor function during emptying of a liquid meal from the stomach in the conscious pig. *J Physiol (Lond)* 422: 523–538, 1990.

